JOURNAL OF MATERIALS SCIENCE 26 (1991) 648 - 654

The effects of thermal fatigue on a SiC fibre/aluminosilicate glass composite

L. P. ZAWADA
WRDC/MLLN, Wright Patterson Air Force Base, Ohio 45433-6533, USA
R. C. WETHERHOLD
Department of Mechanical and Aerospace Engineering, State University of New York, Buffalo, New York 14260, USA

The thermal fatigue (TF) of ceramic matrix composites introduces stresses within the composite due to the thermal expansion mismatch of fibre and matrix; this will affect the lifetime and dimensional stability of the composite. A review of various laboratory TF methods is given, and the controlled, photon heating method used in this research is explained. A Nicalon fibre/glass matrix composite was subjected to rapid, controlled TF from 250 to 700 °C and 250 to 800 °C under no load and dead load conditions in order to illustrate a variety of elastic and inelastic cyclic strain conditions. To characterize simple environmental exposure at elevated temperature, ageing experiments were also run. After TF, the surfaces of the composites were characterized using SEM for evidence of thermal damage and microcracking. The composites were then tested for flexural strength. Results show that the tensile modulus after TF testing remains constant, and that dimensional changes are slight, except near any local hot spots. The 700 °C maximum TF specimens showed appreciably greater embrittlement and lower strength than the 800 °C maximum TF specimens. Observations in the SEM of the surfaces of the 700 °C specimens showed little matrix flow of the type which could decrease oxygen infiltration. Greater matrix flow was observed for the 800 °C specimens. Thermally aged specimens gave results similar to those for the TF experiments.

1. Introduction

The applications for which ceramic matrix composite (CMC) materials are being considered usually involve high homologous temperature creep conditions, and the temperature conditions are often cyclic in nature, producing thermal fatigue (TF). In monolithic ceramics, TF is not a significant problem, unless temperature gradients arise. In CMC materials, however, stresses are generated internally in the composite under TF, even in the absence of external loads. This is due to the mismatch in the coefficient of thermal expansion (CTE) and other elastic properties between the fibre and matrix. Although the expansion mismatch is usually smaller for CMC than it is for metal matrix composites (MMC), the thermal excursions are expected to be larger. Typical examples for CTE mismatch are $1.4 \times 10^{-6}\,°C^{-1}$ for an SiC/1723 CMC and approximately $4.4 \times 10^{-6}\,°C^{-1}$ for an SiC/Ti_3Al MMC. The thermal loads may be combined with mechanical loads to produce thermomechanical fatigue (TMF). Almost all of the currently considered applications for CMC materials involve a duty cycle where TMF conditions exist. In fact, the TMF conditions start with the initial cool-down from fabrication. The TMF cycle for composites cannot, unfortunately, be separated into a "bithermal fatigue" regime [1] as in monolithic materials, because the internal stresses arise during any thermal excursion. The information we must have to increase confidence in the structural design use of CMCs which experience TMF encompasses three areas:

(i) instantaneous elastic properties, for flexibility and vibration;
(ii) deformation, including inelastic deformation, for dimensional stability;
(iii) damage mechanisms and metrics, for lifetime and reliability.

In searching for a model material for TF laboratory testing, we need it to exhibit all of the aspects of typical CMC behaviour. At room temperature, both the fibre and matrix are elastic and brittle. At use temperatures, the fibre is primarily elastic, while the matrix is viscoelastic. The CMC system selected here is a Nicalon* fibre/aluminosilicate glass matrix composite, which has the advantage of being very "tunable" in its cyclic response. That is, the matrix inelastic behaviour is a strong function of temperature, so that the proportions of elastic and inelastic strain may be controlled by proper selection of the maximum cyclic temperature changes. The maximum cyclic temperatures for this work were chosen with regard to the strain point and annealing point of the glass matrix. In this paper,

*TM Nippon Carbon Co. Ltd., Japan.

0022–2461/91 $03.00 + .12

the basic changes which occur during TF are identified using cyclic temperatures as a qualitative tool. Results will include microstructural characterization as well as mechanical behaviour.

Another important aspect of the testing programme in this research compared with previous high-temperature testing research lies in the nature of the TF testing. In referring to the many different types of TF test stations currently used for CMC materials, it is convenient to separate the testing methods into two categories: burner rigs and furnaces. The typical burner rig test station can take many forms. The simpler test stations consist of an oxyacetylene torch for heating, and compressed air for cooling [2–4]. More intricate testing stations involve directing the exhaust of small turbine engines directly at a test specimen [5]. There are several distinct advantages in using burner rig test stations. Rapid heating rates can be attained, and it is possible to create an environment similar to what the components may see in service. One can also adjust the composition of the flame to create unique corrosive or oxidizing conditions. High gas velocity and flame impingement result in vibration and erosion actions similar to turbine engine combustor environments. However, the uniformity and control of temperature during a thermal cycle is very difficult. Often high thermal gradients exist through the thickness of the specimen, and the heating–cooling rates tend to be highly non-linear.

Thermal fatigue test stations using a furnace approach include resistance-heated ovens [6], fluidized beds [7], and susceptors [8]. The simpler methods involve placing either a single specimen or multiple specimens into a furnace and cycling the temperature of the furnace. To speed up the period of the cycle, one can place the specimens into a hot furnace and allow the specimens to reach isothermal conditions. The specimens are then simply removed from the furnace and allowed to air cool or are placed into another furnace at a different temperature. Such test stations are easy and inexpensive to build, have very good temperature control with no overshoot of maximum and minimum limits, and can be used to screen many new CMC systems quickly. However, in order to simulate duty cycle conditions, the heating cycle must be more rapid and linear than that which conventional ovens can provide. It is strongly desirable to maintain well-defined and controlled heating and cooling rates throughout the entire cycle. Therefore, it is an additional aim of this research to refine and quantify the rapid, controlled TF test conditions possible using photon heating techniques [9, 10].

2. Experimental procedure

Composite fabrication was performed as follows. The SiC fibres were Nicalon (Nippon Carbon Co., Yokohama, Japan) ceramic grade fibres which came with a protective type-M sizing. The fibres have an average diameter of 12.5 μm and came as a tow of 500 fibres wound on a spool. As-received fibres were cleaned of their sizing by passing the fibre tow through a burn-off furnace. The fibre tow was then pulled through a glass slurry mixture of glass frit, distilled water, and an organic binder. The glass frit is an alkaline earth aluminosilicate, code 1723, from Corning Glass Works. The infiltrated fibre tows were wound on to an eight-sided mandrel, lamp dried, and cut into 10 cm × 10 cm laminae. These laminae were stacked in a unidirectional laminate $[0_{10}]_T$ in a graphite die. Two 6.3 mm (0.25 in.) thick graphite spacer plates were placed between three separate stacks of laminates. The whole assembly was then densified in a vacuum hot press at elevated temperature and pressure. This single hot press run produced three uniform plates. The plates were 1.6 mm thick and had a fibre volume fraction of approximately 45%. All of the specimens for this study were sectioned from these three plates to minimize processing variations.

The thermal fatigue test fixture is a "rigid grip" system already described elsewhere [9]. The specimen is gripped by superalloy water-cooled grips, and the gauge section is photon heated by eight 1000 W quartz bulbs in a four above–four below configuration. The two lamp bodies are positioned 7 mm from the top and bottom surfaces of the specimen. The bulbs are controlled by a Microcon 823 P.I.D. multiloop controller according to readings from four K-type thermocouples bonded to the specimen by a ceramic adhesive. Use of the Microcon and thermocouples allows for four independently controlled temperature zones. Considerable effort is required to correctly place the thermocouples on the specimen so as to ensure good temperature control with no local hot spots. The optimum thermocouple placement was identified first on trial specimens, and once determined, was used for all subsequent testing.

As mentioned earlier, the matrix inelastic behaviour is a strong function of temperature. The aluminosilicate glass has a strain point of 665 °C and an annealing point of 710 °C. The maximum cyclic temperatures were chosen as 700 and 800 °C, as these temperatures are below and above the annealing point of the glass. The minimum temperature for both of the TF cycles was chosen as 250 °C. Attempts to cool specimens below this temperature resulted in non-linear cooling rates and much longer cycle periods. The cycling period was 5 min for a 250 to 700 °C cycle, and 6 min for a 250 to 800 °C cycle. The cycle periods were chosen to provide linear heating and cooling rates of 1.5 °C sec^{-1} for both cycles. Fig. 1 shows a typical temperature–time trace for a 250 to 800 °C TF experiment. The specimen dimensions were typically 100 mm by 5 mm by 1.6 mm thick, with 67 mm between the grips, and a temperature-controlled gauge section approximately 40 mm long.

Specimens were statically loaded in tension by applying a fixed displacement using a horizontal Schenk Mechanical testing machine in which the TF apparatus is aligned. Because there is some flexibility in the load train of the Schenk machine, the loads experience minor reductions over a thermal cycle (− 14 MPa). Three loads were considered: 138 MPa, a nominal load of 27 MPa, and a true zero load achieved by gripping one end of the specimen and supporting but not gripping the other end. All tests

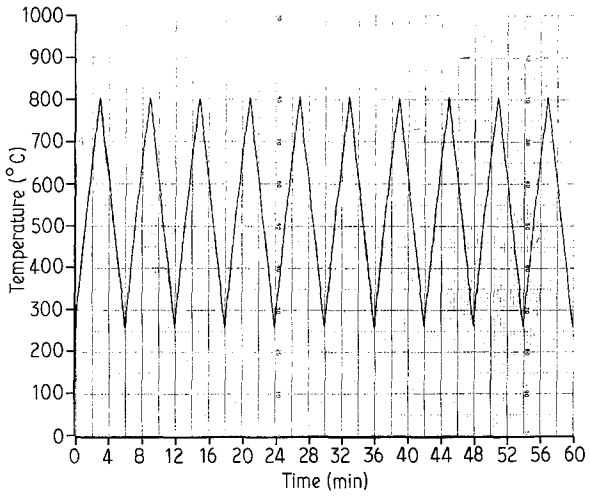

Figure 1 Temperature–time trace for a 250 to 800 °C thermal fatigue test on an SiC/1723 unidirectional composite.

were conducted in laboratory air. Strain measurements were performed using a high-temperature quartz rod extensometer with a 12.7 mm gauge length. The extensometer was mounted horizontally, which greatly reduces the contact forces required to keep the extensometer in contact with the specimen. Placement of the extensometer was on the specimen edge at the centre of the length. The strain signal was filtered, conditioned, and amplified for graphical presentation.

A central issue in thermal fatigue testing is the uniformity of temperature in the gauge section at any instant. The optimal placement of thermocouples (TC) used for control must be determined to avoid local hots spots. The temperature profile was checked by using extra thermocouples in addition to the four used for control. In addition to thermocouple placement, it was found that the specimen width is crucial to proper temperature uniformity. Specimens approximately 5 to 6 mm (0.2 to 0.25 in.) wide offered acceptable uniformity (+15 to −10 °C), while early trial specimens 12 mm wide exhibited unacceptable variability (+27 to −20 °C).

Thermal ageing experiments were carried out in order to separate the effects of a simple exposure at elevated temperature from the effects of thermal fatigue. The specimens were placed on a platform in the centre of a standard box oven for 16 h. Temperatures of 650 and 800 °C were selected, because either temperature should allow any interfacial reaction to proceed [11–14]. However, the 650 °C thermal age is below the glass straining temperature while substantially greater matrix flow is expected at 800 °C.

3. Results and discussion

Overall mechanical property changes were evaluated before and after TF. The width and thickness of specimens were measured at five pre-set locations to determine any gross dimensional changes. For the 700 °C TF specimens, the dimensions did not change. The 800 °C TF specimens demonstrated little dimensional change, except at two locations on the specimen which were visibly identified as "hot spots." The temperature profile at maximum temperature of a typical 250 to 800 °C TF test specimen is shown in Fig. 2. In the figure, one can see that the hot spots are actually located between the outside bulb and its neighbouring bulb. It was thought, initially, that any hot spots would occur directly under a bulb, but this was not the case. A reading from an extra thermocouple placed at a hot spot location indicated a maximum temperature of 815 °C. At hot spots, the thickness change was of the order of 6% for two of the specimens and 12% for the third specimen. The dimensional changes appeared to be from gas generation and bubble formation in the matrix. This was not a problem as none of the failures initiated from this region when the specimens were tested for residual strength. Thickness measurements after TF were difficult to make due to the presence of residual cement from bonding the thermocouples to the specimen.

A further question of interest for dimensional stability is the cyclic strain, as measured by the average strain and total strain for a TF cycle. Results for an 800 °C TF test under load (138 MPa), where creep should be maximum, are shown in Fig. 3. The strain is observed to be stable, indicating that a temperature of 800 °C is not quite high enough for gross composite viscous flow. Tensile moduli were measured in tension using an extensometer during loading and unloading of the specimen within the TF apparatus, while the residual strengths were measured at room temperature in an 80 mm outer span four-point flexure fixture. Results are presented in Table I; one replicate per condition was used unless otherwise noted.

The specimens with high strength (959 to 1124 MPa) failed in a jagged, brushy manner in the fixture gauge section, while the low strength specimens (145 to 210 MPa) failed near the quarter span points in a flat cleavage-type fracture. For the high-strength specimens, the failure proceeds as a series of semi-independent fibre fractures through the specimen until an irregular critical path can link up diagonally across the transverse direction. Once the cracks link up, there is a sudden drop in load, but the specimen remains as one piece. A typical high-strength failure is shown in Fig. 4. The specimen is shown just after

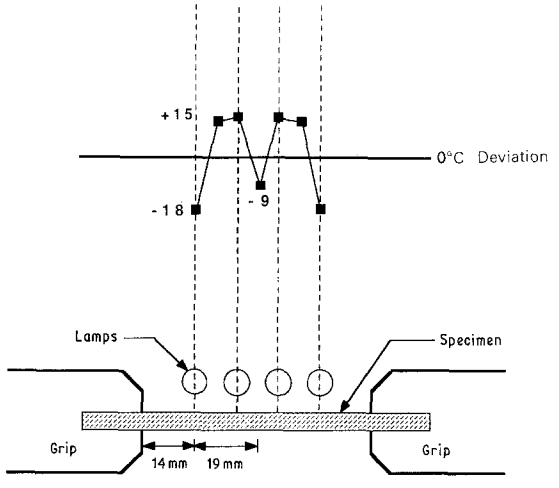

Figure 2 Temperature profile of a 250 to 800 °C thermal fatigue test specimen when cycled to the maximum temperature of 800 °C.

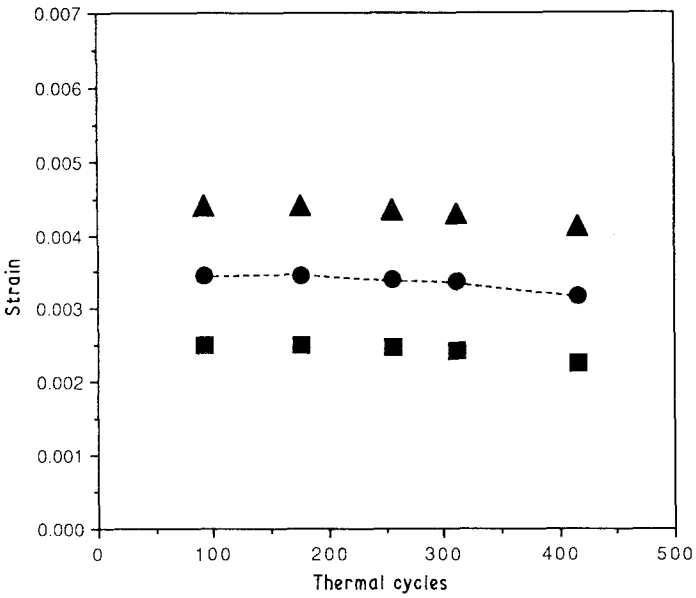

Figure 3 Cyclic strain versus cycle count for a 250 to 800 °C, 138 MPa static load, thermal fatigue test: (▲) maximum, (●) average, (■) minimum strain.

TABLE I Summary of modulus and strength measurements for unidirectional SiC/1723 thermal fatigue specimens tested in flexure (80 mm outer span four-point fixture)

Conditions	Tensile modulus (GPa)		Flexural strength (MPa/replicates)
	before TF	after TF	
Control (as-fabricated)	–	–	1124/3
16 h exposure, 800 °C	–	–	959/4
16 h exposure, 650 °C	–	–	160/2
250 to 700 °C, 500 cycles, 138 MPa static load	158	158	210
250 to 700 °C, 500 cycles, 27 MPa static load	152	141	150
250 to 700 °C, 500 cycles, 0 MPa static load	–	–	250
250 to 800 °C, 450 cycles, 138 MPa static load	150	–	138
250 to 800 °C, 500 cycles, 27 MPa static load	163	158	168
250 to 800 °C, 500 cycles, 0 MPa static load		–	145

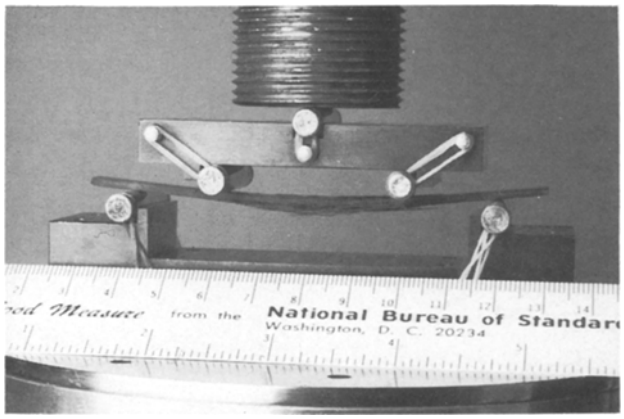

Figure 4 Brushy failure mode of a high-strength SiC/1723 unidirectional composite tested in four-point flexure.

failure while still in the flexure fixture. One can observe the high density of cracks on the tensile half of the specimen and the absence of cracks on the compressive half. However, all of the low-strength TF specimens failed by a single crack propagating straight across the thickness. During failure, the specimens broke into two pieces. Observations of the fracture

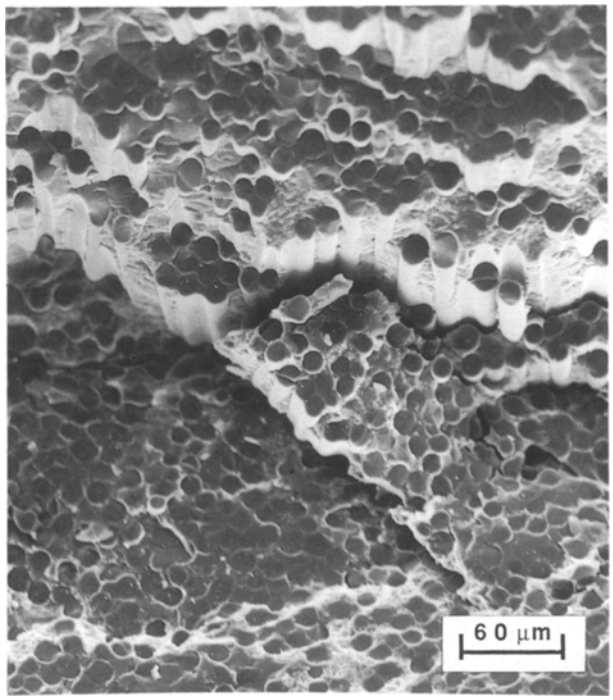

Figure 5 Fracture surface of a 250 to 700 °C TF specimen which exhibited flat fracture and low flexural strength.

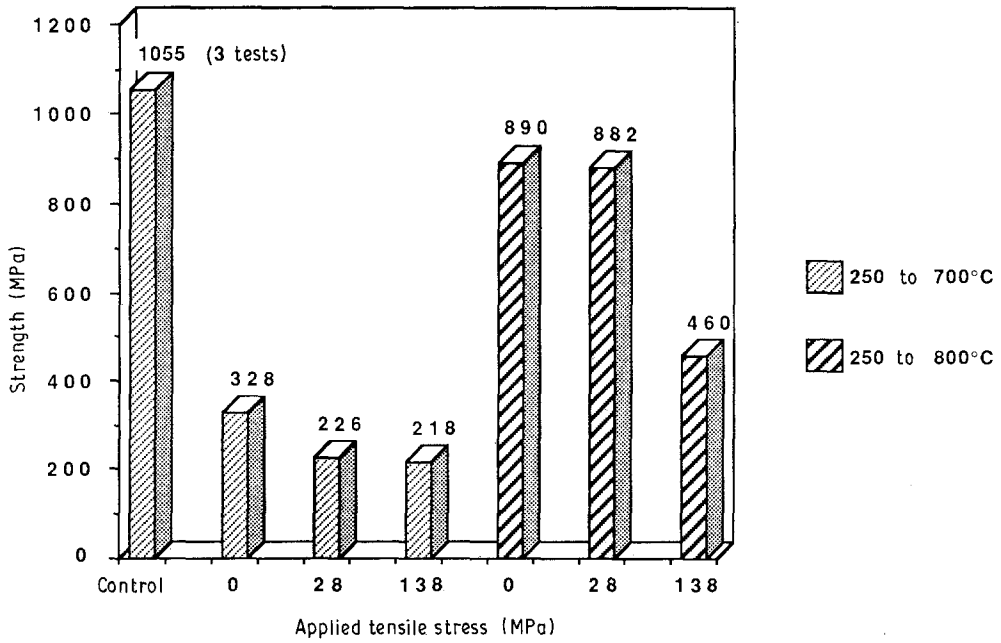

Figure 6 Graphical representation of strength measurements for unidirectional SiC/1723 thermal fatigue specimens. Results are for control specimens, 250 to 700 °C, and 250 to 800 °C TF specimens tested on a four-point flexure fixture (outer span 40 mm).

surface revealed no fibre pull-out and a flat cleavage-type fracture surface similar to that observed in failed monolithic glass. A photomicrograph of a typical low-strength fracture surface is shown in Fig. 5. It is worth noting that the specimens exposed to 650 °C for 16 h had an average residual strength of only 160 MPa, yet they did not fail in a cleavage manner. The failure mode was made up of many diagonally running cracks. The difference in failure modes for each of the test conditions makes direct comparison of the results difficult.

Following the low-strength failures observed after TF, it is observed that the failure location (near the quarter span loading nose) falls where there is a substantial thermal gradient between the heated gauge section and the cooled grips. Temperatures at the failure locations were typically less than 650 °C. As mentioned above, all of the observed low-strength failures are completely brittle in nature. There is an impression that intermediate temperatures, and not high temperatures, lead to faster embrittlement and lower strengths (see Table II). Because the TF specimens seem unaffected in their central gauge area by the 80 mm fixture flexure testing, it was decided to retest the central zone of each specimen in a 40 mm flexure fixture. The flexural strength results are given in Table II and presented graphically in Fig. 6.

The control specimens are seen to possess similar strengths and failure modes in either 80 or 40 mm lengths. All three of the 700 °C TF specimens exhibited a moderate increase in strength and a cleavage-type failure. The failure mode is shown schematically in Fig. 7a. The crack would initiate as a straight transverse crack running across the tension side of the

TABLE II Summary of strength measurements for SiC/1723 unidirectional specimens retested on a four-point flexure fixture with an outer span of 40 mm

Test conditions	Flexural strength (MPa/replicates)
Control (as-fabricated)	1055/3
250 to 700 °C, 500 cycles 138 MPa static load	218
250 to 700 °C, 500 cycle 27 MPa static load	226
250 to 700 °C, 500 cycles 0 MPa static load	328
250 to 800 °C, 450 cycles 138 MPa static load	460
250 to 800 °C, 500 cycles 27 MPa static load	882
250 to 800 °C, 500 cycles 0 MPa static load	890

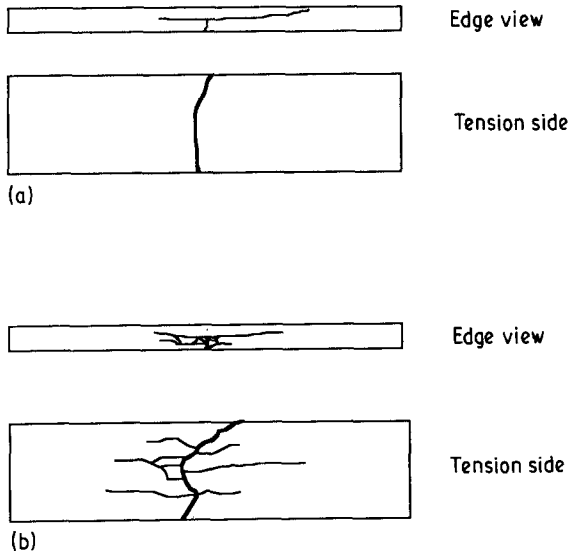

Figure 7 Schematic representation of the different failure modes observed for thermal fatigue specimens tested on a four-point flexure fixture (outer span 40 mm). Specimen (a) was cycled from 250 to 700 °C while (b) was cycled from 250 to 800 °C.

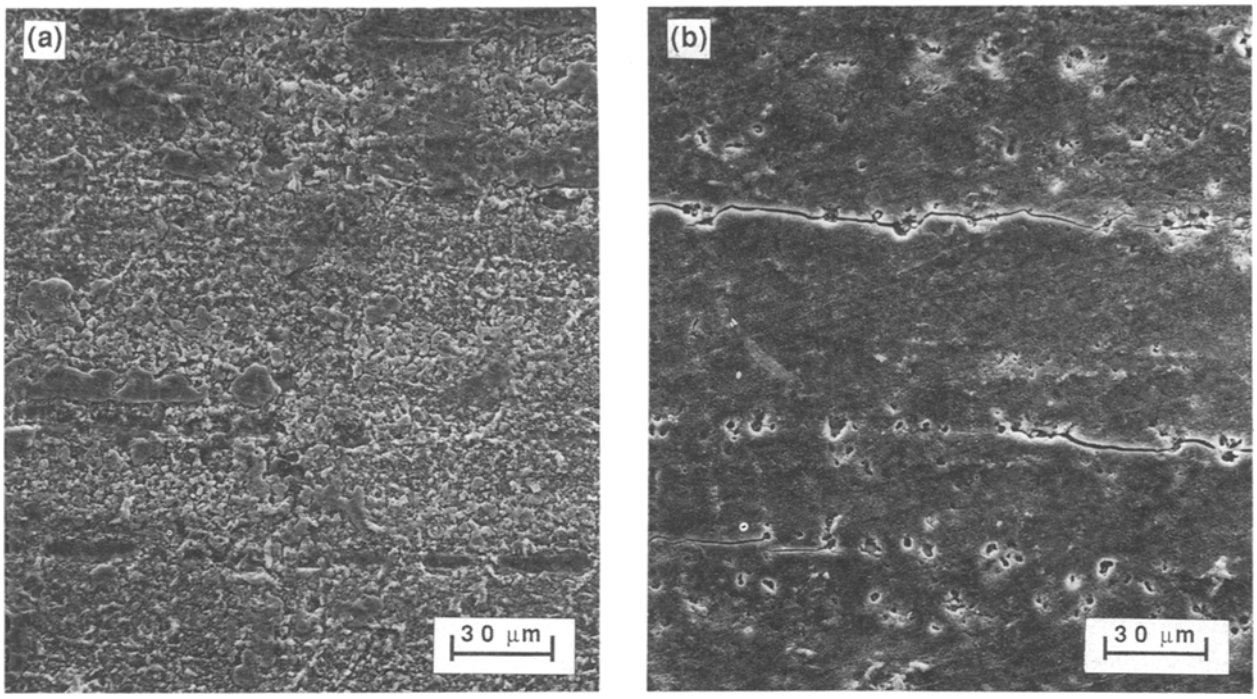

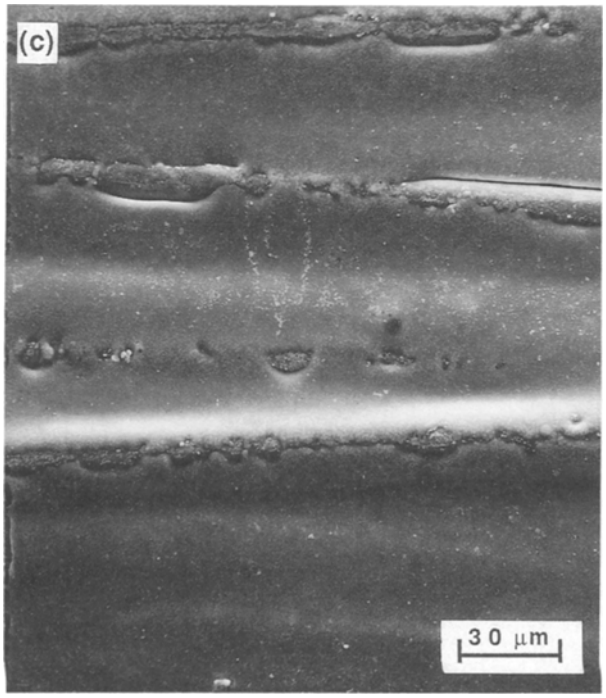

Figure 8 Surface characteristics for a unidirectional SiC/1723 composite: (a) as hot-pressed, (b) after cycling to 700 °C, and (c) after cycling to 800 °C.

specimen. Once formed, it would run sharply up through the thickness of the specimen to the neutral axis. When it reached the neutral axis it would deflect and form a delamination crack running mostly parallel to the fibres. The delamination crack would work its way towards the top surface in compression resulting in final failure and two pieces. The 800 °C TF specimens show a rather greater strength increase and a more desirable failure mode. As shown schematically in Fig. 7b, the crack on the tension side of the specimen was jagged and ran somewhat diagonally across the surface. Crack propagation through the specimen was characterized by many secondary cracks and severe matrix damage, which was most heavily localized near the neutral axis. At the neutral axis the crack would deflect and become a delamination crack. The failure surfaces on the tension side showed brushy failure and, the specimen remained intact.

It thus appears that the 800 °C TF specimens retain their strength better. It was thought that the retainment of strength might possibly be due to the matrix flow's helping to seal surface and subsurface cracks and thus protecting the interior of the composite from oxygen infiltration. To confirm this damage prevention or self-healing mechanism, the appearance of the surfaces of the specimens is of interest during TF. The as-fabricated surface appears somewhat irregular (Fig. 8a). After cycling to 700 °C, the surface appearance becomes somewhat smoother, and cracks have formed parallel to those fibres which lie at the surface: no transverse cracks were seen (see Fig. 8b). Specimens cycled to 800 °C show a smooth surface, and the matrix has flowed around the fibres (see Fig. 8c). In addition, one can see the blunted and rounded remains of what appear to have been cracks running along fibres near the surface similar to those seen in Fig. 8b.

Both the 650 °C thermal age specimens and the 700 °C TF specimens exhibited rapid oxidation behaviour and loss in strength. Such results reveal that for these test conditions the oxidation behaviour overwhelms any thermal fatigue effects which might occur. In contrast, the 800 °C TF tests demonstrated little effect from thermal cycling.

4. Conclusion

CMC specimens were thermally cycled, with a rapid, linear, controlled temperature profile. The compliance of the specimens does not change appreciably during cycling, while the strengths decrease with a truly

brittle fracture mode. Subsequent testing of the thermally controlled section showed that the 700 °C TF specimens had a very low strength, while 800 °C TF specimens retained most of their strength. Given the observations of smoothing of surface features in 800 °C specimens, it appears that a higher cycling temperature may actually improve strength retention. It is postulated that the higher temperature causes the viscosity of the glass matrix to lower sufficiently to allow it to flow at stress concentrations and crack openings, which may in turn decrease the oxygen infiltration and thus lessen embrittlement. The surface would still incur some degradation, but the bulk interior of the composite would be protected. This high-temperature improvement occurs under both TF and thermal ageing conditions.

Degradation of glass-ceramic composites due to environmental attack is well documented [12–18]. The loss in strength is attributed to two mechanisms. Oxidation of the carbon-rich fibre–matrix interface burns out the carbon. At the same time the SiC fibre oxidizes resulting in an amorphous SiO_2 surface layer and CO_2 generation [12, 13, 19]. The strong interfacial bond created contributes to brittle composite behaviour. In contrast, there is limited documentation on composite systems which demonstrate a preventative degradation mechanism which is more active at elevated temperatures than intermediate temperatures. Prewo [18] has shown that for an LAS-II matrix composite fatigued above the proportional limit, maximum environmental degradation took place when the composite was exposed in air at 600 °C. When similar specimens were exposed in air at 900 °C, they retained a significant amount of residual strength. No mechanism for the superior 900 °C behaviour was presented.

In carbon–carbon composites, the matrix oxidation threshold is approximately 370 °C. Therefore, the carbon–carbon community has relied on various types of coatings for oxidation protection. However, most of the coatings are deposited at elevated temperature, and microcrack during cooling. Microcracks formed by thermal mismatch stresses between the coating and substrate require the incorporation of sealants to provide protection. Current sealants are borate glass-formers or boron-based glassy sealants which, at elevated temperatures, melt and fill in cracks. This type of sealing mechanism can start to operate as low as 650 °C [11]. It is postulated that there is a similar type of sealing mechanism occurring for the SiC/1723 CMC system investigated in this study.

References

1. G. R. HALFORD, M. A. McGAW, R. C. BILL and P. D. FANTI, "Bithermal Fatigue, A Link Between Isothermal and Thermomechanical Fatigue", in ASTM STP 942, "Low cycle fatigue" (American Society for Testing and Materials, Philadelphia, Pennsylvania, 1988) p. 625.
2. C. F. JOHNSON and D. L. HARTSOCK, in "Thermal Response of Ceramic Turbine Stators in Ceramics for High Performance Applications", edited by J. J. Burke, A. E. Gorum, and R. N. Katz (Brook Hill, Chestnut Hill, Massachusetts, 1974) p. 549.
3. G. D. QUINN, "Characterization of Turbine Ceramics After Long-Term Environmental Exposure", AMMRC TR80-15 (1980): available NTIS, ADA17463.
4. J. WARREN and B. COWLES, "A Simplified Thermomechanical Fatigue Test Method", ASME, Paper Number 86-GT-20, January 1986.
5. C. METZLOFF, "Hot Cell Testing", in Proceedings of the High-Temperature Testing of Materials: 2 to 13 November 1986, Institute for Defense Analyses Memo Report M278, December 1986.
6. R. WARREN, L. O. K. LARSSON, P. EDSTROM and T. JANSSON, in "Progress in Science and Engineering of Composites", edited by T. Hayashi, K. Kawada and S. Umekawa (Japanese Society for Composite Materials, Tokyo, 1982) pp. 1419.
7. M. A. H. HOWES, "Evaluation of Thermal Fatigue Resistance of Metals using the Fluidized Bed Technique, Fatigue at Elevated Temperatures", ASTM STP 520 (American Society for Testing and Materials, Philadelphia, Pennsylvania, 1973) pp. 242–54.
8. K. NAKANO, L. ALBINGRE, R. PAILLER and J. M. QUENISSET, *J. Mater. Sci. Lett.* **4** (1985) 1046.
9. G. A. HARTMAN, L. P. ZAWADA and S. M. RUSS, "Techniques for Elevated Temperature Tensile Testing of Advanced Ceramic Composite Materials", in Proceedings of the Fifth Annual Hostile Environment and High Temperature Measurements Conference, (Society for Experimental Mechanics Bethel, CT, 1988) pp. 31–8.
10. G. A. HARTMAN III, *J. Test. Eval.* **13** (1985) 363.
11. J. R. STRIFE and J. E. SHEEHAN, *Amer. Ceram. Soc. Bull.* **67** (1988) 369.
12. K. M. PREWO, G. K. LAYDEN, E. J. MINFORD and J. J. BRENNAN, "Advanced Characterization of SiC Fiber Reinforced Glass-Ceramic Matrix Composite", ONR Report no. R85-916629-1 under ONR Contract No. N00014-81-C-0571, June 1985.
13. J. J. BRENNAN, "Interfacial Chemistry and Bonding in Fiber Reinforced Glass and Glass-Ceramic Matrix Composites", in Ceramic Microstructures '86, MRS **21**, Ed J. A. Pask, A. G. Evens (Plenium Pub. 1987) 387.
14. T. MAH, M. G. MENDIRATTA, A. P. KATZ and K. S. MASDIYASNI, *Amer. Ceram. Soc. Bull.* **66** (1987) 304.
15. T. MAH, M. MENDIRATTA, A. KATZ, R. RUH and K. MAXDIYASNI, *J. Amer. Ceram. Soc.* **68** (1985) 248.
16. R. L. STEWART, K. CHYUNG, M. P. TAYLOR and R. F. COOPER, in "Fracture Mechanics of Ceramics", Vol. 7, edited by R. C. Bradt *et al.* (Plenum, New York, 1986) pp. 33–51.
17. J. F. MANDELL, D. H. GRANDE and J. JACOBS, "Tensile Behavior of Glass/Ceramic Composite Materials at Elevated Temperatures", J. of Engineering for Gas Turbines and Power, Transactions of the ASTM, **109** (1987) 267.
18. K. M. PREWO, *J. Mater. Sci.* **22** (1987) 2695.
19. E. BISCHOFF, M. RUHLE, O. SBAIZERO and A. G. EVANS, *J. Amer. Ceram. Soc.* **72** (1989) 741.

Received 16 October 1989
and accepted 20 March 1990